ACS APPLIED MATERIALS & INTERFACES

Research Article

www.acsami.org

Incorporation of a Clot-Binding Peptide into Polythiophene: Properties of Composites for Biomedical Applications

Georgina Fabregat,[†,‡] Bruno Teixeira-Dias,[†,‡] Luis J. del Valle,[†] Elaine Armelin,[†,‡] Francesc Estrany,[‡,§] and Carlos Alemán*[,†,‡]

[†]Departament d'Enginyeria Química, ETSEIB, Universitat Politècnica de Catalunya, Avda. Diagonal 647, Barcelona E-08028, Spain

[‡]Center for Research in Nano-Engineering, Universitat Politècnica de Catalunya, Campus Sud, Edifici C', C/Pasqual i Vila s/n, Barcelona E-08028, Spain

[§]Departament d'Enginyeria Química, EUETIB, Universitat Politècnica de Catalunya, Comte d'Urgell 187, Barcelona E-08036, Spain

Supporting Information

ABSTRACT: Biocomposites formed by a pentapeptide (CREKA), which recognizes clotted plasma proteins, entrapped into the poly(3,4-ethylenedioxythiophene) (PEDOT) matrix have been prepared using three very different procedures. X-ray photoelectron spectroscopy analyses indicate that PEDOT-CREKA films, prepared by chronoamperometry in basic aqueous solution (pH = 10.3) and deposited onto a PEDOT internal layer, present the higher concentration of peptide: one CREKA molecule per six polymer repeat units. The surface of this bilayered system shows numerous folds homogeneously distributed, which have been exhaustively characterized by scanning electron microscopy and atomic force microscopy. Indeed, the morphology and topography of such bilayered films is completely different from those of biocomposite-prepared acid aqueous and organic solutions as polymerization media. The impact of the entrapped peptide molecules in the electrochemical properties of the conducting polymer has been found to be practically negligible. In contrast, biocompatibility assays with two different cellular lines indicate that PEDOT-CREKA favors cellular proliferation, which has been attributed to the binding of the peptide to the fibrin molecules from the serum used as a supplement in the culture medium. The latter assumption has been corroborated examining the ability of PEDOT-CREKA to bind fibrin. The latter ability has been also used to explore an alternative strategy based on the treatment of PEDOT-CREKA with fibrin to promote cell attachment and growth. Overall, the results suggest that PEDOT-CREKA is appropriated for multiple biomedical applications combining the electrochemical properties of conducting polymer and the ability of the peptide to recognize and bind proteins.

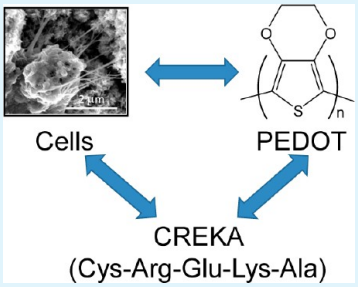

KEYWORDS: *cell proliferation, composite, electroactive polymer, fibrin, peptide*

INTRODUCTION

Conducting polymer (CP) coatings have been shown to improve the charge transfer characteristics of conventional metal electrodes, and biological assays have revealed that proteins and cells preferentially adhere to coated electrodes.[1−4] As a consequence, many CPs have been used in tissue engineering applications, even though research efforts have been mainly concentrated on polypyrrole (PPy), poly(3,4-ethylenedioxythiophene) (PEDOT), and their derivatives.[5] Some extracellular matrix biomolecules, especially peptides, are known to support cell attachment and growth when incorporated into CPs or used as a coating.[6−15]

The incorporation of peptides can be carried out using different approaches. The most frequent is the incorporation of anionic peptides as dopant agents of the CPs,[5−15] which is achieved through the incorporation of the biomolecule into the monomer medium used for the polymerization process. Unfortunately, this particular class of dopants may produce significant undesirable changes in the bulk properties of the CP, reducing the electrical conductivity, the electroactivity, the electrochemical stability, etc. Another emerging noncovalent approach to modify CPs for biomedical applications is based on the use of peptides with binding specificity, which are selected from phage display libraries. For example, surface modification with Arg-Gly-Asp (RGD) of chlorine-doped PPy with chlorine peptide promotes the PC12 cell adhesion in serum-free media, whereas no adhesion is observed on unmodified surfaces.[12] An advantage of this surface approach is that, apparently, it should not modify the intrinsic properties of the CP and could be used with a wide range of different biomolecules that do not need to be negatively charged. In addition to the dopant and noncovalent entrapment approaches, modification of CPs via covalent bonds has been also explored. Multiple techniques have been used, for example: the modification of the β-position on PPy to create strong disulfide bonds with the Cys of Arg-Gly-Asp-Cys (RGDS), enhancing osteoblast adhesion[13,14] and the modification of the surface to immobilize peptides through covalent bonds, which have been successfully used for different

Received: December 2, 2013
Accepted: July 22, 2014
Published: July 29, 2014

biomedical applications (e.g., immobilize nerve growth factor[15] and promote cellular proliferation[16]).

Over the last years, Ruoslahti and co-workers have identified a series of tumor-homing peptides by using in vivo screening of peptide libraries.[17,18] Among the homing peptides discovered by this procedure exists a linear peptide that contains only five amino acids with sequence Cys-Arg-Glu-Lys-Ala (CREKA).[17,18] This pentapeptide, which recognizes fibrin−fibronectin complexes, was used to design a self-amplifying nanoparticle delivery system.[19] Iron oxide nanoparticles coated with this peptide accumulate in tumor vessels, where they induce additional local clotting and thereby produce new binding sites for more nanoparticles. This amplification system enhanced homing of the nanoparticles in a mouse tumor model without causing clotting or other obvious side effects in the body. Although self-amplified tumor accumulation produced enhancement of tumor imaging, significant inhibition of tumor growth was not obtained. Determination of the bioactive conformation of CREKA through computer-aided modeling tools[20,21] led to engineer a series of analogues by targeted replacements in Arg and Glu, which were replaced by the corresponding N- and C^{α}-methylated amino acids.[22] CREKA analogue nanoparticles were combined with nanoparticles coated with another tumor-homing peptide (Cys-Arg-Lys-Asp-Lys-Cys) and nanoparticles with an elongated shape (nanoworms). Treatment of mice with prostate cancer with multiple doses of these nanoworms induced tumor necrosis and highly significant reduction in tumor growth.[22]

Modification of CPs by introducing CREKA analogues, which due to their unique properties could extend the biomedical applications of these materials, is highly desirable. In this work we focus on the most appropriated approach and conditions for the incorporation of this peptide into the polymer matrix as well as on their impact on the CP properties. As the synthesis of the above-mentioned CREKA analogues involves an important chemical effort, which is essentially related with the preparation of nonproteinogenic amino acids, the parent peptide CREKA has been used for the investigations reported in this work. However, as the charge distribution is the same in CREKA as in its N- and C^{α}-methylated analogues (i.e., all these peptides are cationic with two positively charged amino acids and only one negatively charged), the former should be considered a good model. The CP used in this work to immobilize CREKA is PEDOT, which has been frequently used in biomedical applications (e.g., DNA and glucose biosensors[23,24] and bactericide protein immobilization[25]).

The main aim of this work is to investigate the conditions required for the preparation of bioactive platforms based on the modification of PEDOT with CREKA. To extend this platform in the near future to antitumoral CREKA derivatives, we have addressed the synthetic conditions, structural and physical properties, biocompatibility, and bioactivity of modified PEDOT, hereafter referred to as PEDOT-CREKA. Within this context, in this contribution we have evaluated three different approaches to modify PEDOT with CREKA. The influence of the peptide on the morphology, topography, and electrochemical properties has been established by comparing PEDOT with PEDOT-CREKA. Furthermore, the biocompatibility of PEDOT-CREKA has been evaluated by analyzing the cellular activity through adhesion and proliferation assays. Finally, to prove that the peptide retains the bioactive conformation, the ability to bind fibrin of PEDOT-CREKA has been studied.

METHODS

Materials. CREKA peptide with >98% of HPLC purity was purchased from GenScript USA Inc. The source for the rest of the materials is described in the Supporting Information (SI).

Synthesis. Both anodic polymerization and electrochemical assays were performed with an Autolab PGSTAT302N equipped with the ECD module (Ecochimie, The Netherlands) using a three-electrode compartment cell under nitrogen atmosphere (99.995% pure) at room temperature. Steel AISI 316 sheets of 1 cm^2 in area were used as working and counter electrodes. To prevent interferences during the electrochemical assays, the working and counter electrodes were cleaned with acetone before each trial. The reference electrode was a Ag|AgCl electrode containing a KCl saturated aqueous solution [offset potential versus the standard hydrogen electrode, E^0 = 0.222 V (V) at 25 °C], which was connected to the working compartment through a salt bridge containing the electrolyte solution.

Although all PEDOT-CREKA composites reported in this work were prepared by anodic polymerization, different approaches that differ in the procedure and/or experimental conditions were employed to identify the material with optimum properties.

(1). PEDOT-CREKA Films Produced in Organic Environment. The anodic compartment of the cell was filled with 10 mL of a 0.01 M EDOT solution in acetonitrile containing 0.1 M $LiClO_4$ as supporting electrolyte and 1 mg/mL of CREKA aqueous solution, while the cathodic compartment was filled with 10 mL of the same electrolyte solution. Films were prepared by chronoamperometry (CA) under a constant potential of 1.40 V, which was identified as the optimum value for the polymerization of EDOT in acetonitrile,[26] using a polymerization time θ = 200 s (i.e., films obtained using smaller polymerization times were very fragile and difficult to handle). The experimental conditions used for the preparation of PEDOT films used as blank were identical to those of PEDOT-CREKA with the exception of the anodic compartment, which was filled with 5 mL of 0.01 M EDOT solution in acetonitrile containing 0.1 M $LiClO_4$ as supporting electrolyte and 5 mL of ultrapure Milli-Q water. Hereafter, films prepared using these conditions are denoted PEDOT-CREKA-(Acn+wat) and PEDOT(Acn+wat).

(2). PEDOT-CREKA Films Produced in a Basic Aqueous Environment. All films were prepared by CA using an aqueous medium with pH = 10.3 (adjusted with NaOH) and a constant potential of 1.10 V, which was identified as the optimum potential for the polymerization of EDOT in water.[27] Preliminary assays indicated that films obtained by direct electrodeposition of the composite onto the steel electrode were very fragile and difficult to handle for characterization and application assays. To overcome this limitation, the preparation of PEDOT-CREKA films was afforded using a new approach based on a two-step process. Initially, the steel electrode was coated with PEDOT. For this purpose, the anodic compartment was filled with 10 mL of a 20 mM EDOT monomer aqueous solution containing 10 mM SDBS as supporting electrolyte, while the cathodic compartment was filled with 10 mL of the same electrolyte solution. The polymerization time selected for the electrodeposition of this coating layer was θ = 10 s (i.e., different trials using θ = 20 and 30 s did not improve the electrochemical properties). After this, a new layer of PEDOT-CREKA composite was electrodeposited onto the surface of the PEDOT layer. This was achieved by filling the anodic compartment with a generation solution identical to that mentioned above for the first layer but containing 1 mg/mL of CREKA peptide. The applied potential and the polymerization time were 1.10 V and θ = 20 s, respectively. PEDOT films used as the blank were prepared employing experimental conditions identical to those described above, even though two different systems were considered: (1) single-layered films obtained using a polymerization times of 10, 20, and 30 s (i.e., the polymerization times used for the individual layers of the bilayered system and its sum) and (2) bilayered films obtained without CREKA (i.e., two PEDOT layers prepared using polymerization times of 10 and 20 s). Hereafter, composite and blank films prepared using these conditions are denoted PEDOT/PEDOT-CREKA(basic-wat), PEDOT(basic-wat), and PEDOT/PEDOT(basic-wat), respectively.

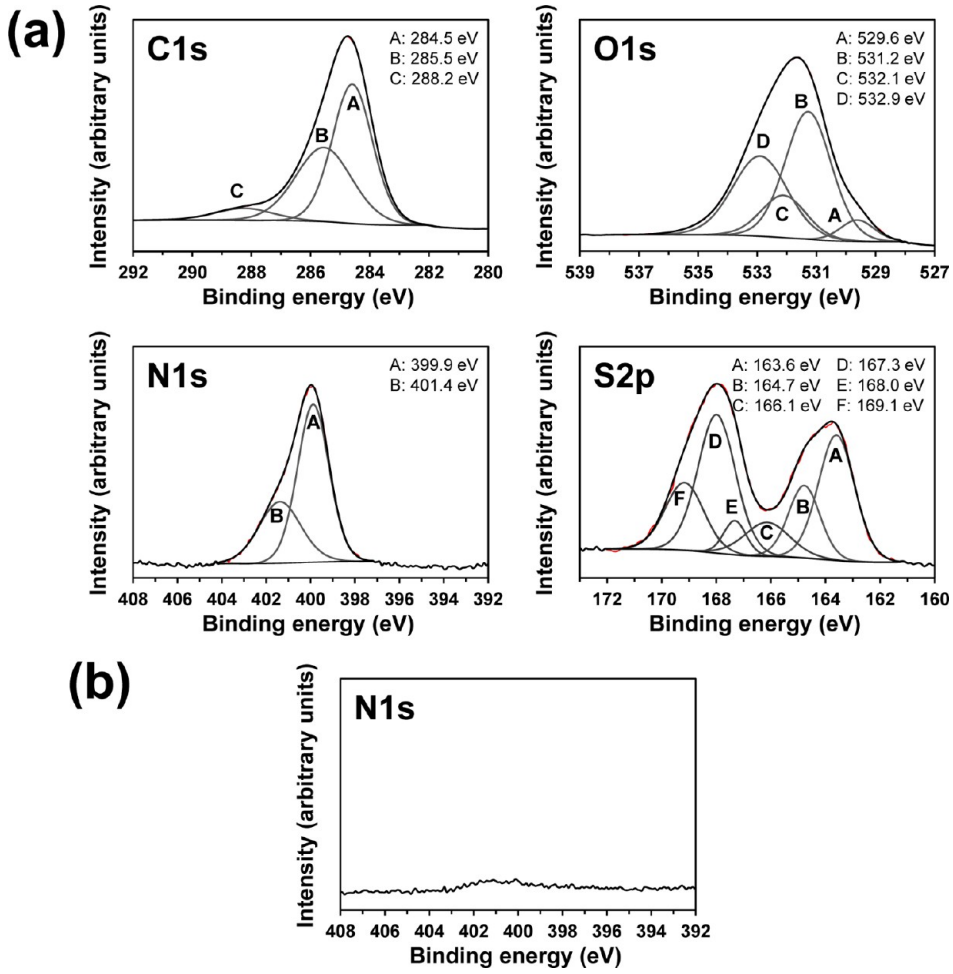

Figure 1. (a) High-resolution XPS spectra for PEDOT/PEDOT-CREKA(basic-wat): C 1s, O 1s, N 1s, and S 2p regions. (b) N 1s region of the XPS spectra recorded for the internal PEDOT layer before the electrodeposition of the PEDOT-CREKA composite. Peaks from deconvolution are displayed in all cases.

3). PEDOT-CREKA Films Produced in an Acid Aqueous Environment. The anodic compartment of the cell was filled with 5 mL of an aqueous medium with pH = 5.4 (adjusted with HCl) containing 0.01 M EDOT, 0.1 M SDBS, and 1 mg/mL of CREKA peptide. The cathodic compartment was filled with 10 mL of the same electrolyte solution. Films were generated by CA using a constant potential of 1.10 V and a polymerization time of 10 s, which was the minimum time required to obtain a complete coverage of the surface. For the preparation of the PEDOT films used for comparison, which were obtained under the same experimental conditions, the CREKA peptide was not included in the generation medium. The composite and blank films produced in this environment have been denoted PEDOT-CREKA(acid-wat) and PEDOT(acid-wat), respectively.

Characterization. The SI provides details of the equipment and conditions used for characterization by FTIR spectroscopy, X-ray photoelectron spectroscopy (XPS), high-performance liquid chromatography (HPLC), scanning electron microscopy (SEM), atomic force microscopy (AFM), contact profilometry, and cyclic voltammetry.

Biological Assays. *Cell Adhesion and Proliferation Test.* In vitro adhesion and proliferation assays were performed using two different cellular lines of adherent growth: (i) cells HEp-2 (human line derived from an epidermoid carcinoma of larynx) and (ii) cells DU145 (human line derived from a prostate carcinoma). HEp-2 and DU145 have an epithelial morphology. The tissue culture polystyrene (TCPS) plate has been used as a control substrate.

Cells were plated in 25 cm^2 tissue flasks and grown in Dulbecco's Modified Eagle's Medium (DMEM) supplemented with 10% fetal bovine serum (FBS), penicillin G (100 U/mL), and streptomycin (100 mg/mL). Cultures to evaluate cellular adhesion and proliferation were incubated during 24 h and 7 days, respectively. Details of the procedures used for the culturing and seeding of the cells in adhesion and proliferation assays are provided in the SI. Viable cells were determined using the MMT [3-(4,5-dimethylthiazol-2-yl)-2,5-diphenyltetrazolium] method. Analyses were carried out using the cell adherence density in each sample in comparison to the control (%, relative of control). All experiments were repeated at least three times.

Fibrin Recognition. Analyses to examine the adsorption of fibrin onto the surface of PEDOT and PEDOT-CREKA composites were performed according to the protocol described in the SI.

RESULTS AND DISCUSSION

Chemical Composition. The biocomposites were examined by FTIR and XPS spectroscopies. The FTIR spectra (not shown) of PEDOT-CREKA samples prepared by the different procedures described above (see Methods section) and of their PEDOT counterparts were qualitatively similar. Unfortunately, the entrapped peptide was not clearly detectable in the biocomposites. Thus, the amide I (1700−1600 cm^{-1}) and amide II (1600−1500 cm^{-1}) regions, which arise primarily from the C═O stretching vibration and the coupling between the N−H in-plane bending and C−N stretching modes, respectively, and the N−H (free: 3500−3300 cm^{-1}; hydrogen bonded: 3350−3070 cm^{-1}) were not clearly recognizable because of the overlapping with the band associated with the

thiophene ring (C═C and C−C stretching) and water (O−H stretching) bands. Regarding the latter, it should be mentioned that hydration occurred despite samples being stored 2 days in a desiccator, evidencing the hydrophilicity of the materials, as was already reported.[28] The rest of the bands were assigned to those typically found in PEDOT:[29−31] C−S stretching (837 cm^{-1}), stretching of the ethylenedioxy group (1141 and 1057 cm^{-1}), and deformation of the ethylenedioxy group (922 cm^{-1}).

Figure 1a displays the high-resolution XPS spectra in the C 1s, N 1s, O 1s, and S 2p regions for PEDOT/PEDOT-CREKA(basic-wat). Before discussing the analysis, it should be mentioned that the peaks of the peptide may be influenced by those of the CP and vice versa, explaining the small deviations found in some peaks with respect to the values reported in the literature.[32−45] Deconvolution of the C 1s peak led to three Gaussian curves that have been attributed to the C−C and C−S bonds of PEDOT and surfactant molecules (284.5 eV), the C−O and C−N of PEDOT and peptide molecules (285.5 eV),[32−34] and the C═O of amide (288.2 eV).[35,36] The O 1s signal consists of four components with the first centered at 532.9 eV, corresponding to the C−O−C bonding in the ethylene bridge.[32,37] The peak centered at 532.1 eV is attributed to the C═O of the amide group,[38] while the component at 531.2 eV is assigned to the COO^- moiety of CREKA and the SO_3^- of SDBS dopant molecules.[38] The component at 529.6 eV is associated with contamination products.[16]

The high-resolution N 1s spectrum, which shows two peaks centered at 399.9 and 401.4 eV, is essential to demonstrate that CREKA is embedded in the PEDOT matrix. Previous studies of CP−peptide composites indicated that peaks comprised between 399 and 400 eV are due to the N−H and N−C═O bonds of the peptides.[16,35,38] The peak centered at 401.4 eV is attributed to the N-terminal free charged amino group.[35,36] The peak assigned to the C−N of the Arg side group, which should appear at 399.2 eV, is overlapped with the lowest energy peak. These observations support the successful incorporation of the peptide into the CP matrix. The high-resolution XPS of the S 2p region for the composite, which is included in Figure 1a, shows the spin-split sulfur coupling, S $2p_{3/2}$ and S $2p_{1/2}$, for the C−S−C bond of the thiophene ring (163.6 and 164.7 eV, respectively), and it is homologous with the positively charged sulfur (i.e., C−S^+−C at 166.1 and 167.3 eV, respectively).[41−44] The components centered at 168.0 (S $2p_{3/2}$) and 169.1 eV (S $2p_{1/2}$) are attributed to the SO_3^- of SDBS (165.1 eV).[45] The component associated with the C−SH of Cys, which is expected at approximately 163.2 eV,[42] is unfortunately overlapped with some other peaks, discrimination not being possible.

High-resolution XPS spectra for PEDOT were reported and discussed in a recent study,[41] and for this reason discussions have not been included in Figure 1. However, to remark on the absence of CREKA signals, Figure 1b displays the spectrum in the N 1s region recorded for the internal PEDOT layer that was used to coat the steel electrode in PEDOT/PEDOT-CREKA(basic-wat) films. Comparison of the N 1s spectra displayed in Figures 1a and 1b corroborates the successful incorporation of CREKA into the CP matrix during the polymerization process. XPS spectra (not shown) recorded for PEDOT-CREKA(Acn+wat) and PEDOT-CREKA(acid-wat) showed the same peaks, the presence of the peptide being demonstrated by the signals detected at the N 1s region.

The number of EDOT units per CREKA peptide molecule in each composite was derived from the *S*/*N* ratio, where *S* refers to the sum of the atomic percent composition associated with the C−S−C and C−S^+−C curves at the S 2p region and *N* is total atomic percent composition of the nitrogen atom. Results indicated that the content of CREKA in PEDOT/PEDOT-CREKA(basic-wat) films is very high with ∼6 EDOT units per CREKA molecule. However, this successful ratio decreases significantly for PEDOT-CREKA(acid-wat) and PEDOT-CREKA(Acn+wat), the number of EDOT units per peptide molecule increasing 1 and 2 orders of magnitude, respectively (i.e., ∼85 and >350 EDOT units per peptide molecule). In general, the atomic compositions obtained by XPS using the conditions described in the Methods section correspond to the surface, the penetration of the X-ray radiation being expected to be of the order of ∼10 nm. As the thickness of PEDOT-CREKA(acid-wat) and PEDOT-CREKA(Acn+wat) films is within the micrometric scale (see next subsection), HPLC analyses were carried out to examine the possible existence of a higher concentration of peptide inside the films (i.e., below 10 nm surface).

HPLC results for CREKA, PEDOT(Acn), and PEDOT-CREKA(Acn+wat) are displayed in Figure 2. Detection of the eluted at 220 nm produced two peaks with retention times of 3.3 and 4.8 min for CREKA (Figure 2a), whereas a single peak with a retention time of 4.8−5.0 min was identified when the eluted was detected at 280 nm (data not shown). We assumed that the peak detected at 280 nm corresponds to a honeycomb structure formed by layers of peptides, as was previously found in other polymer−peptide conjugates.[14,15] The response of PEDOT(Acn) was the same at both 220 and 280 nm, two peaks with different intensities and retention times of 4.8−5.0 and 9.3 min being detected (Figure 2b). The chromatograms of CREKA standards have been followed by absorbance at 220 nm, the linear models for the peaks at 3.3 min (R^2 = 0.9812) and 4.8 min (R^2 = 0.9999) being displayed in the inset of Figure 2a. As a consequence of the excellent correlations between the peak areas and the CREKA concentrations, the two models become indistinguishable.

The concentration of peptide extracted from PEDOT-CREKA(Acn+wat) was determined using the method of the added concentration (Figure 2b). As can be seen, the peaks of CREKA and the peptide extracted from PEDOT-CREKA(Acn +wat) are overlapped. The concentration of peptide in the latter was estimated to be 0.3−0.4%, which corresponds to a PEDOT:CREKA mass ratio of 300:1. This ratio, which corroborates the XPS results, is significantly lower than that used for the electropolymerization of the films. These results indicate that the net positive charge of CREKA, which is removed at basic pH conditions used for the preparation of PEDOT/PEDOT-CREKA(basic-wat) films, makes difficult the entrapment of the peptide into the polymer matrix.

Morphology and Topography. Figure 3a shows the morphology of PEDOT/PEDOT-CREKA(basic-wat) films, which can be described as a relatively compact surface with multiple, relatively prominent, and well-localized folds homogeneously distributed on it. Magnified SEM micrographs reveal differences between the folds and the regions located at the bottom of the surface. Although two such zones consist of the aggregation of pseudospherical granules, the attachment of such elements is clearly more compact at the bottom regions of the surface than at the folds. The average thickness and roughness determined by contact profilometry of PEDOT/PEDOT-

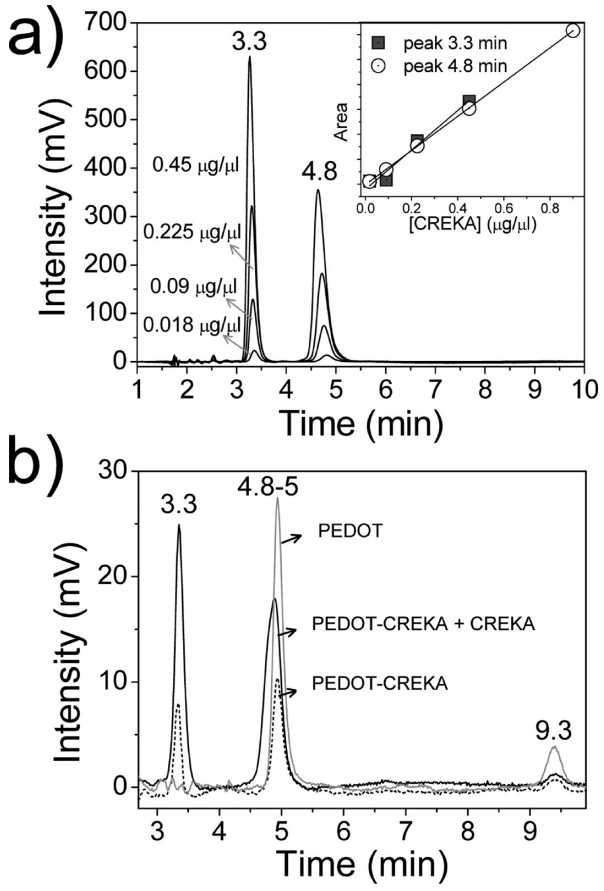

Figure 2. Detection of CREKA in PEDOT-CREKA(Acn+wat) by HPLC. (a) Chromatograms of CREKA at different concentrations show overlapping. The detection was carried out by absorbance at 220 nm. The retention times are indicated over each peak. The inset shows the linear models obtained using the two peaks of CREKA. (b) Chromatograms used to analyze the peptide extracted from PEDOT-CREKA(Acn+wat). The correspondence of peaks was determined by adding a known concentration of CREKA in the extracted sample. A PEDOT extract was used as control to identify the peaks of the conducting polymer.

CREKA(basic-wat) films, including the folds, are 3.8 ± 1.3 μm and 582 ± 24 nm, respectively.

The morphology of PEDOT/PEDOT(basic-wat) films (Figure 3b) is apparently very similar to that described above. Thus, the surface shows many folds homogeneously distributed. However, detailed inspection indicates that such folds are significantly more prominent than those observed in PEDOT/PEDOT-CREKA(basic-wat). The height of the folds, as determined by profilometry, is 7.0 ± 1.4 and 2.5 ± 1.1 μm for PEDOT/PEDOT(basic-wat) and PEDOT/PEDOT-CREKA(basic-wat), respectively. The average thickness and roughness measured for PEDOT/PEDOT(basic-wat) films by profilometry are 7.8 ± 2.9 and 1.4 ± 0.5 μm, respectively.

Inspection of the morphologies reported for PEDOT and PEDOT/PEDOT films produced in acetonitrile[46] evidenced the absence of folds. This feature suggests that the pH and the aqueous solvent used to prepared PEDOT/PEDOT-CREKA-(basic-wat) and PEDOT/PEDOT(basic-wat) may play a crucial role in the formation of the folds displayed in Figures 3a and 3b. To get a further understanding, single-layered PEDOT(basic-wat) films were generated using the same aqueous medium with pH = 10.3 and considering polymerization times of 10 and 20 s, like those used for the internal and external layer of PEDOT/PEDOT(basic-wat), respectively. SEM micrographs of these films are displayed in Figure 3c. As it can be seen, the morphologies are relatively similar to those described for the films produced in acetonitrile, a homogeneous distribution of compact aggregates being observed in the two cases. Furthermore, the size of such aggregates increases with the polymerization time, as was also observed in acetonitrile.[43] Overall, these results indicate that the formation of the folds in PEDOT/PEDOT-CREKA(basic-wat) and PEDOT/PEDOT-(basic-wat) is due to the simultaneous coexistence of three factors rather than two: two polymerization steps, basic pH, and aqueous environment.

Figure 4a displays low- and high-resolution SEM images representative of the overall PEDOT(Acn+wat) morphology. This material presents a heterogeneous surface with multiple flake-like aggregates, which in turn can be described as aggregates of fiber-like sticks. This morphology looks less porous than that of the single-layered films displayed in Figure 3c. Inspection of the SEM images recorded for the PEDOT-CREKA(Acn+wat) surface (not shown) does not reflect any significant difference with respect to those displayed in Figure 4a, suggesting, as occurred for PEDOT/PEDOT-CREKA-(basic-wat), that the entrapped peptide does not alter the surface of the CP.

To ascertain if the peptide affects the surface morphology of the internal side, films were detached from the steel electrodes and coated with an ultrathin layer of carbon. Low- and high-resolution SEM images of the internal side of PEDOT(Acn +wat) and PEDOT-CREKA(Acn+wat) are shown in Figures 4b and 4c, respectively. As can be seen, entrapped CREKA affects both the texture and morphology of PEDOT. The more noticeable results are the homogeneous smooth texture and the practical absence of small nodular outcrops in PEDOT-CREKA(Acn+wat) films, whereas these are frequently and homogeneously present in PEDOT(Acn+wat). These nodules correspond to the typical PEDOT agglomerates previously mentioned, their absence in PEDOT-CREKA(Acn+wat) suggesting a more compact internal surface. The similarity between PEDOT(Acn+wat) and PEDOT-CREKA(Acn+wat) in the external surface morphology has been attributed to the fact that peptide molecules incorporate into the polymer matrix at the first stages of the polymerization process. The average thickness and roughness measured by profilometry for PEDOT-CREKA(Acn+wat) is 2.4 ± 0.5 μm and 429 ± 97 nm, respectively, these values being very similar to those determined for PEDOT(Acn+wat).

Figure 4d shows the morphologies of PEDOT(acid-wat) and PEDOT-CREKA(acid-wat), which are similar to that reported for PEDOT produced in organic media (e.g., acetonitrile solution).[47] Thus, the SEM micrographs reflect a porous structure formed by a dense network of thin fiber-like morphologies connecting small clusters of aggregated molecules that are located at very different levels. In spite of this, it should be noted the occasional apparition of small regions in which the surface becomes smooth (i.e., more compact), which has been attributed to the effect of the acid pH.

Figures 5a–d display AFM micrographs of PEDOT/PEDOT-CREKA(basic-wat) and PEDOT/PEDOT(basic-wat). The topography of the internal PEDOT layer (Figure 5a) can be described as a dense distribution of sharp peaks grouped in clusters (i.e., independent mountain ranges separated by valleys). This surface topography is very similar

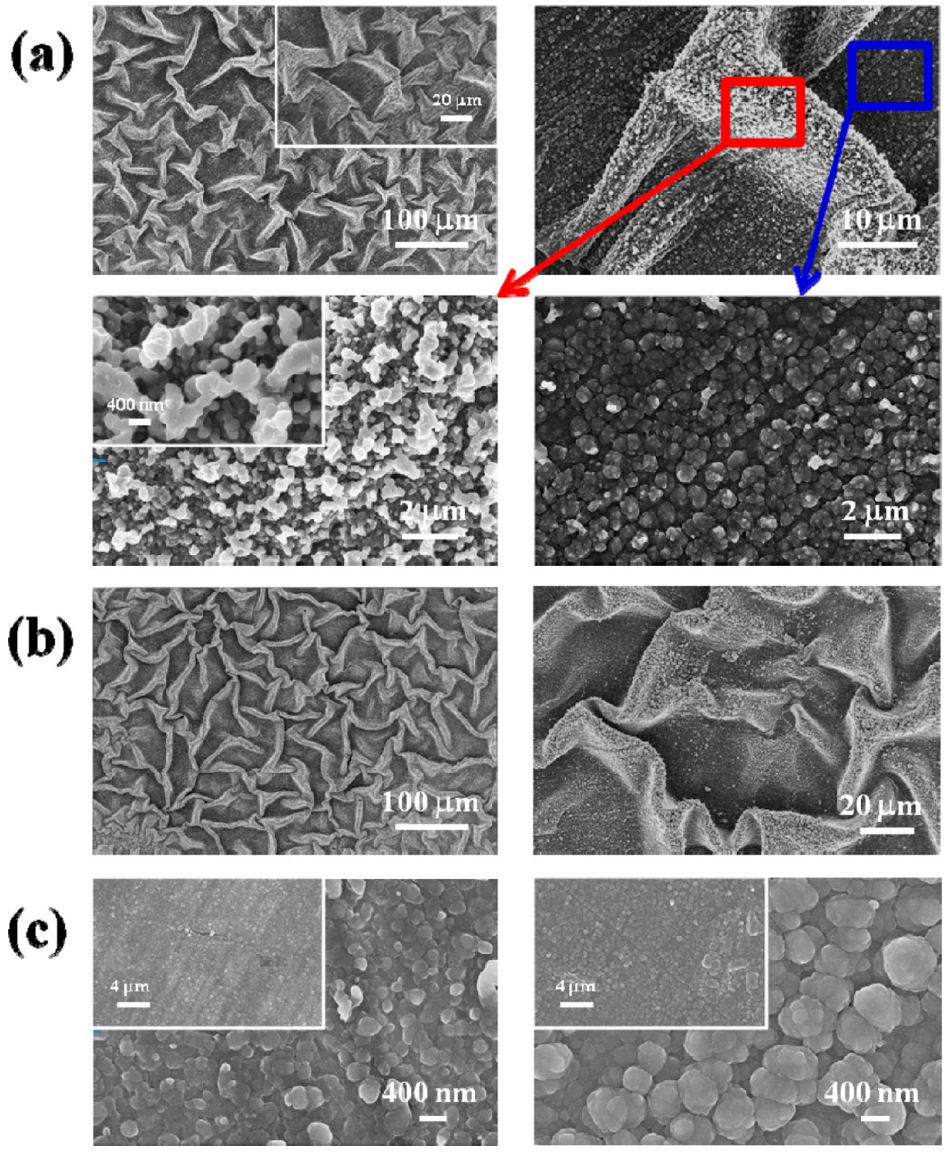

Figure 3. Low- and high-resolution SEM images of: (a) PEDOT/PEDOT-CREKA(basic-wat); (b) PEDOT/PEDOT(basic-wat); and (c) PEDOT(basic-wat) generated using polymerization times of 10 and 20 s (left and right, respectively).

to that obtained for PEDOT films polymerized in acetonitrile at 1.40 V and using 10 s as polymerization time,[48] even though the roughness of the latter (r = 73 ± 6 nm) was slightly higher than that determined in this work for the film generated at 1.10 V and using a basic aqueous environment (r = 29 ± 5 nm). The topographic image of the PEDOT/PEDOT-CREKA(basic-wat) surface (Figure 5b) evidences that the size and number of the clusters observed for the internal layers increases and decreases, respectively, upon the deposition of the composite external layer. Thus, the latter does not provoke a homogeneous growth, in terms of height, of the clusters formed in the internal layer but an aggregation of clusters, which enhances the difference with respect to the plateau regions (i.e., the surface is less leveled). Consistently, the roughness experiences a significant increment (r = 126 ± 28 nm). The surface topography of PEDOT/PEDOT(basic-wat) reveals a similar effect in the absence of CREKA peptide (Figure 5c), even though it is less pronounced. Thus, the size of the aggregates is intermediate between those displayed in Figures 5a and 5b. Similarly, the roughness (r = 74 ± 2 nm) is intermediate between those of the internal PEDOT layer and PEDOT/PEDOT-CREKA(basic-wat). It should be emphasized that the topographies displayed in Figures 5b and 5c correspond to a bottom surface region rather than to the folds observed by SEM for the two bilayered systems (see Figures 3a and 3b). Figure 5d displays the AFM image (25 μm × 25 μm) of one of the folds observed in PEDOT/PEDOT-CREKA(basic-wat). The height of the fold, which has been estimated using the cross-sectional profile of the topography image (included in Figure 5d), is ~3.3 μm, this value being in good agreement with the value obtained using cross-sectional SEM (3.8 μm).

The AFM image displayed in Figure 5e for PEDOT-CREKA(acid-wat) evidences a surface topography very similar to that of the internal PEDOT layer of PEDOT/PEDOT-CREKA(basic-wat) films. This consists of a relatively dense distribution of sharp peaks that are grouped forming small clusters. As PEDOT chains exclusively involve α–α linkages (i.e., the β positions of the thiophene ring are occupied by the fused dioxane ring), the clusters are attributed to the formation

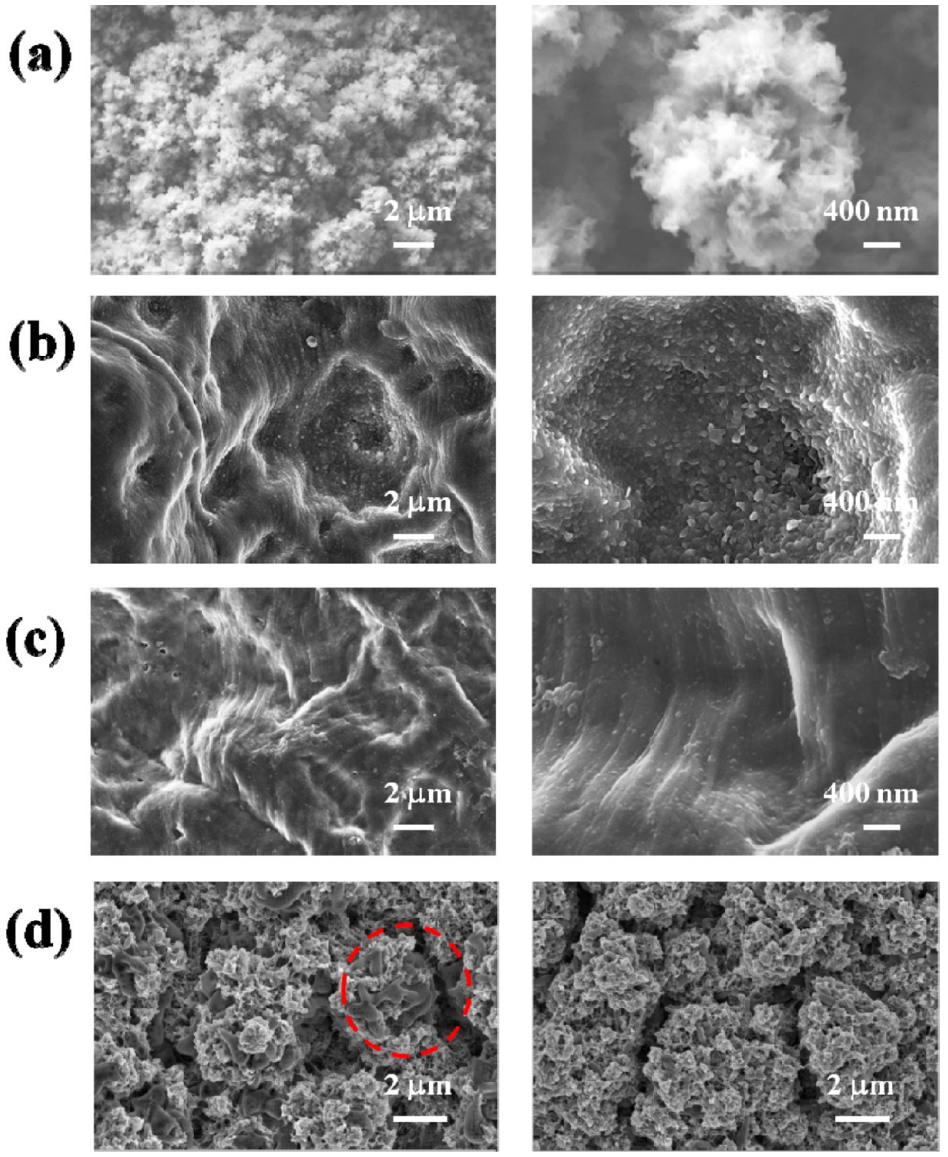

Figure 4. Low- and high-resolution SEM images (left and right, respectively) of (a) the external surface morphology of PEDOT(Acn+wat) and the internal surface morphology of (b) PEDOT(Acn+wat) and (c) PEDOT-CREKA(Acn+wat). Internal surfaces of PEDOT(Acn+wat) and PEDOT-CREKA(Acn+wat) films were coated with an ultrathin layer of carbon. (d) SEM micrographs of PEDOT(acid-wat) and PEDOT-CREKA(acid-wat) (left and right, respectively). The red circle shows a smooth region.

of compact molecular aggregates of linear chains that are stabilized by the dopant agent. The roughness of PEDOT-CREKA(acid-wat) (r = 51 ± 6) is intermediate between those of the internal layer of PEDOT/PEDOT-CREKA(basic-wat) and PEDOT produced in acetonitrile using $LiClO_4$ as supporting electrolyte (r = 29 ± 5 and 73 ± 6 nm, respectively).[48] Finally, the AFM images of PEDOT-CREKA-(Acn+wat) (Figure 5f) and PEDOT(Acn+wat) (not shown) are very similar, resembling those reported for micrometric PEDOT films produced in acetonitrile using a constant potential of 1.40 V, a polymerization time higher than 100 s, and $LiClO_4$ as supporting electrolyte.[48] The topography consists of a reduced number of compact and, simultaneously, large blocks of aggregated polymer chains emerging over flat regions. Also, the surface roughnesses of PEDOT-CREKA(Acn +wat) and PEDOT(Acn+wat) (r = 392 ± 34 and 381 ± 29 nm, respectively) are higher than those for the rest of the films described in Figure 5.

Charge Store Ability and Electrochemical Stability. The cyclic voltammograms of PEDOT/PEDOT(basic-wat) and PEDOT/PEDOT-CREKA(basic-wat) in a physiological environment (0.1 M PBS, pH= 7.4), which were recorded in the potential range from −0.40 to 0.80 V, are displayed in Figure 6a. Comparison with the voltammogram obtained for the PEDOT internal layer of such two-layered films, which is included in Figure 6a, indicates that the maximum anodic current density (j_{max}), which is reached at the reversal potential, increases significantly upon the incorporation of the second layer (i.e., from 0.75 to ∼1.0 mA·cm^{-2}, which represents an increment of ∼35%). Furthermore, the second layer provokes an increment of the electroactivity. More specifically, the ability to store charge increases by 20% and 17% when the second layer is deposited onto the internal layer in PEDOT/PEDOT(basic-wat) and PEDOT/PEDOT-CREKA(basic-wat), respectively. Accordingly, the electrochemical properties of PEDOT/PEDOT(basic-wat) and PEDOT/PEDOT-

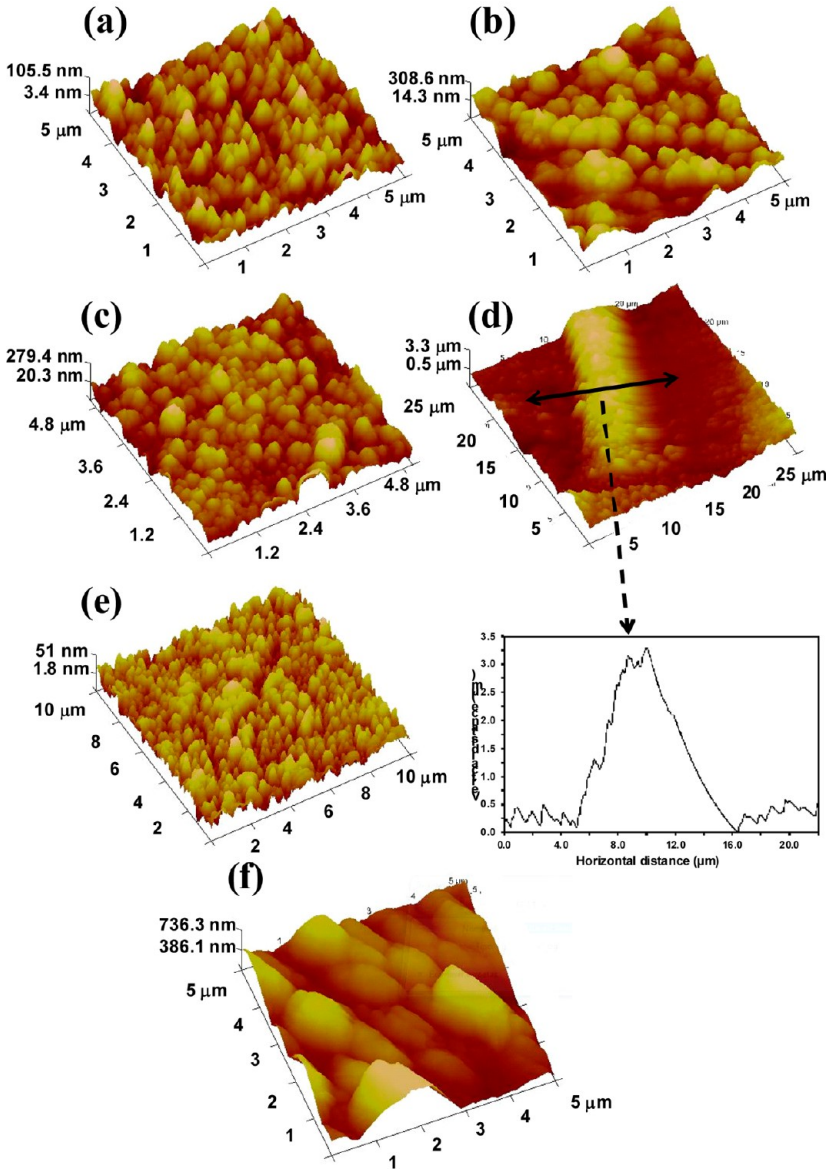

Figure 5. AFM micrographs (3D topography) of the: (a) internal PEDOT layer of PEDOT/PEDOT-CREKA(basic-wat) and PEDOT/PEDOT(basic-wat); (b) surface of PEDOT/PEDOT-CREKA(basic-wat) (bottom surface region); (c) surface of PEDOT/PEDOT(basic-wat) (bottom surface region); (d) surface of PEDOT/PEDOT-CREKA(basic-wat) (region with fold); (e) surface of PEDOT(acid-wat); and (f) surface of PEDOT-CREKA(Acn-wat). The cross-sectional profile of the topography image is included in (d).

CREKA(basic-wat) are very similar, indicating that the influence of the entrapped CREKA peptide molecules is significantly lower than that produced by the bilayered structure of the film. This behavior is fully consistent with those previously reported for different PEDOT-containing multilayered films produced in organic solvents.[46,47]

To evaluate the electrochemical stability of the films produced in a basic aqueous environment, control voltammograms have been compared with those recorded after five oxidation−reduction cycles in PBS, which are included in Figure 6a. The loss of ability to store charge is higher for two-layered films than for the internal PEDOT layer. Thus, the electroactivity of PEDOT/PEDOT(basic-wat) and PEDOT/PEDOT-CREKA(basic-wat) decreases 12% and 18% after five consecutive redox cycles, while that of the internal PEDOT layer decreases by only 9%. This result is in agreement with previous observations, which reflected that the interfaces between layers found in multilayered films have a negative effect on the electrostability.[49] Despite its relatively high concentration, CREKA does not affect the redox capabilities of PEDOT as is reflected by the considerable resemblance between PEDOT/PEDOT(basic-wat) and PEDOT/PEDOT-CREKA(basic-wat) in terms of both electroactivity and electrostability.

Figure 6b compares the control voltammograms and the voltammograms after five consecutive redox cycles in 0.1 M PBS (pH = 7.4) recorded for PEDOT(acid-wat) and PEDOT-CREKA(acid-wat). As was expected, the small concentration of peptide incorporated into the polymeric matrix generated in an acid aqueous environment does not provoke significant changes in terms of electroactivity and electrostability. Thus, the ability to store charge of PEDOT(acid-wat) and PEDOT-CREKA-(acid-wat) is practically identical, whereas the loss of electroactivity after five cycles is of 16% and 14% for the former and

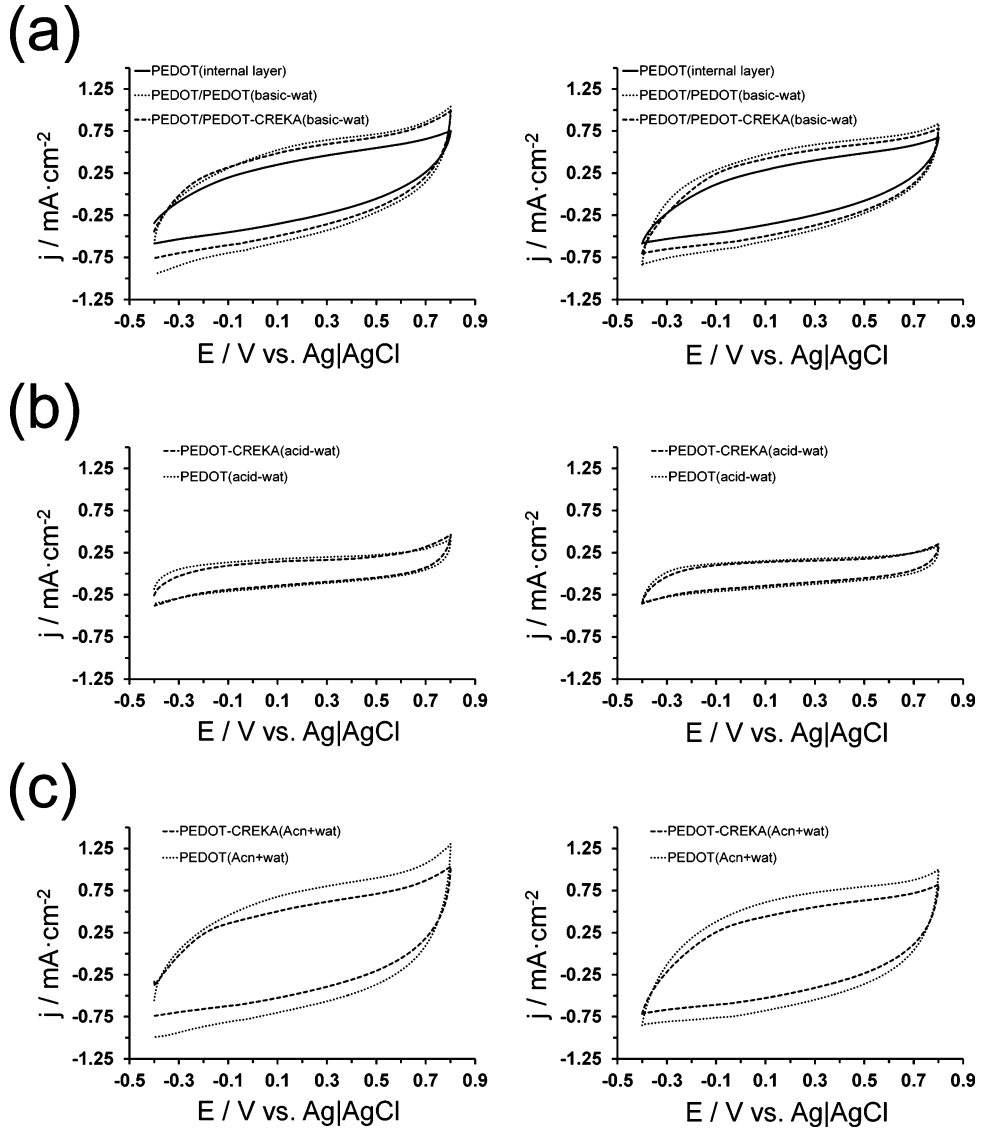

Figure 6. Initial control voltammogram (left) and voltammogram after five consecutive oxidation−reduction cycles (right) in 0.1 M PBS (pH = 7.4) of: (a) internal PEDOT layer, PEDOT/PEDOT(basic-wat), and PEDOT/PEDOT-CREKA(basic-wat); (b) PEDOT(acid-wat) and PEDOT-CREKA(acid-wat); and (c) PEDOT(Acn+wat) and PEDOT-CREKA(Acn+wat).

the latter, respectively. Furthermore, comparison of the voltammograms displayed in Figures 6a and 6b indicates that the electroactivity of the films obtained in a basic environment is ∼65% higher than that of films generated in an acid medium.

The most electroactive films are those generated in a mixture of acetonitrile and water using $LiClO_4$ as supporting electrolyte (Figure 6c). Thus, the ability to store charge of PEDOT(Acn +wat) and PEDOT-CREKA(Acn+wat) is 28% and 5% higher than that of PEDOT/PEDOT(basic-wat) and PEDOT/ PEDOT-CREKA(basic-wat), respectively. In this case, the substitution of a small amount of perchlorate dopant anions by CREKA peptides has a noticeable impact on the electroactivity, which was not observed in PEDOT-CREKA-(acid-wat) when a small concentration of SDBS dopant was replaced by peptide molecules. This feature should be attributed to the excellent properties of the perchlorate anion as the dopant agent, which in turn are due to its small size, high mobility, and charge concentration.[23,50] The loss of electroactivity after five redox cycles amounts to 15% and 18% for PEDOT(Acn+wat) and PEDOT-CREKA(Acn+wat), indicating that their electrochemical stability is very similar to that of PEDOT(basic-wat) and PEDOT/PEDOT-CREKA(basic-wat).

Biocompatibility. The abilities of PEDOT/PEDOT-CREKA(basic-wat), PEDOT-CREKA(acid-wat) PEDOT-CREKA(Acn+wat), and the corresponding PEDOT substrates without CREKA to cellular adhesion and proliferation were compared by considering two different cellular lines: HEp-2 and DU-145. These carcinogenic cells were selected due to their fast growth. Quantitative results of cellular adhesion assays are displayed in Figure 7a, TCPS (or culture plate) being used as a control substrate. Results indicate that the peptide does not provoke any effect in the adhesion of the cells, which was found to be similar in all cases to that obtained for the control TCPS. After 7 days of culture, the cellular activity was re-evaluated. Results, which are displayed in Figure 7b, show a similar number of viable cells per unit of material for TCPS, PEDOT-CREKA(acid-wat), PEDOT-CREKA(Acn+wat), PEDOT(acid-wat), and PEDOT(Acn+wat). Although the entrapment of CREKA in the polymer matrix was expected to favor cellular adhesion and/or proliferation through the binding to the fibrin

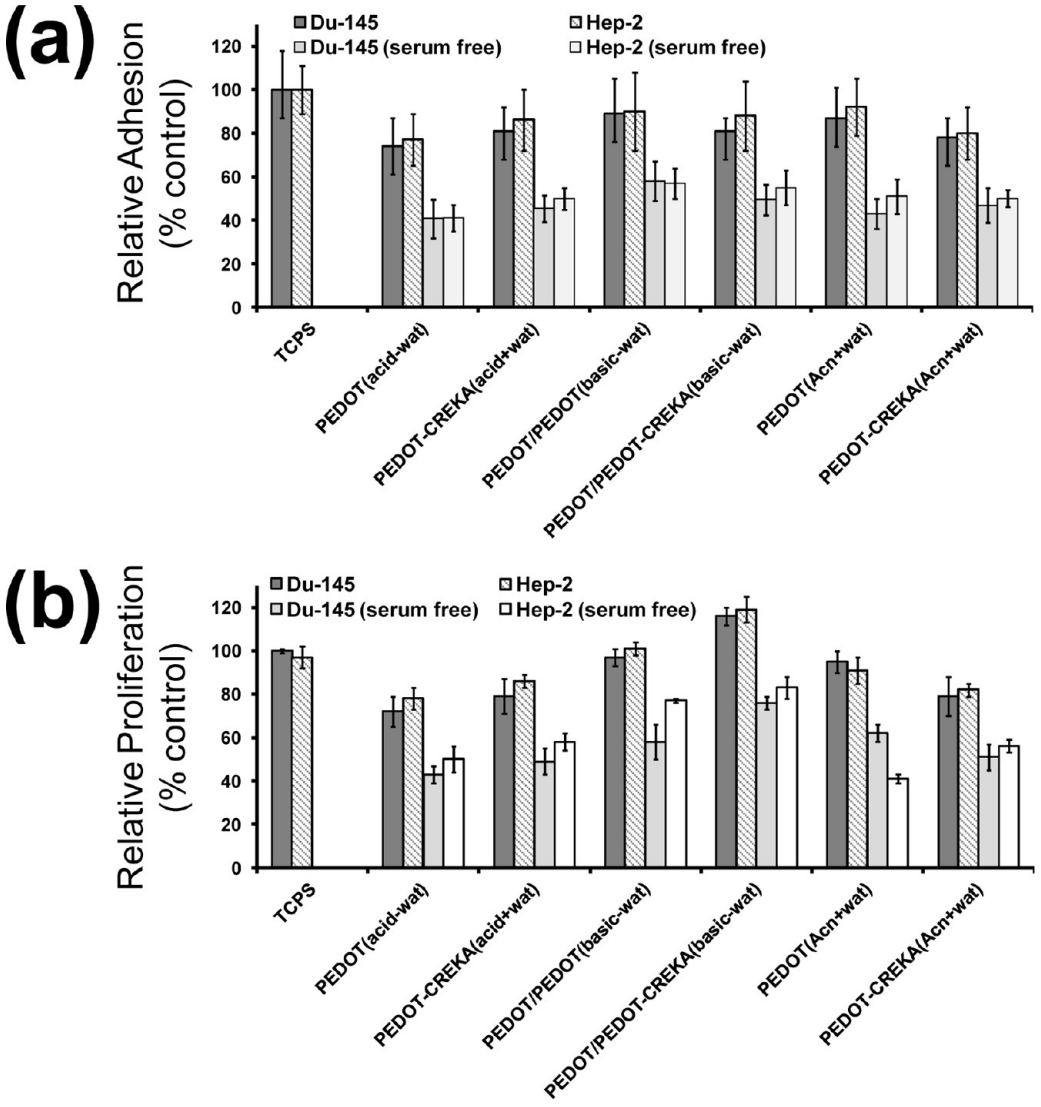

Figure 7. Cellular adhesion (a) and cellular proliferation (b) on the surface of PEDOT(acid-wat), PEDOT-CREKA(acid-wat), PEDOT/PEDOT(basic-wat), PEDOT/PEDOT-CREKA(basic-wat), PEDOT(Acn+wat), and PEDOT-CREKA(Acn+wat). TCPS was used as a control substrate. DU-145 and HEp-2 cells were cultured during 24 h (adhesion assay) and 7 days (proliferation assay). Fetal bovine serum was added or not to the supplement used for the culture medium, results obtained for cells cultured in the serum-free media being explicitly labeled. The experiments were performed using six samples for each substrate.

molecules from the serum used as supplement in the culture medium, the peptide concentration was, unfortunately, too low in PEDOT-CREKA(acid-wat) and PEDOT-CREKA(Acn+wat) (i.e., 0.3−0.4%).

In contrast, the number of proliferated cells per area of PEDOT/PEDOT(basic-wat) and, especially, PEDOT/PEDOT-CREKA(basic-wat) increases appreciably with respect to the number of adhered cells per area of the same material. The fact that such improvement is observed for both bilayered films indicates that enhancement of the proliferation must be partially attributed to the high surface roughness achieved when the polymerization medium consists of a basic aqueous solution. However, the percentage of proliferated cells is ∼20% higher for PEDOT/PEDOT-CREKA(basic-wat) than for PEDOT/PEDOT(basic-wat) evidencing that the concentration of peptide in the former is high enough to promote cell viability.

Figure 8 shows SEM micrographs adhered and subsequently proliferated on the surface of PEDOT(Acn+wat) and PEDOT-CREKA(Acn+wat) films. The cellular mechanism operating for the adhesion of the cells onto the surface of the two bilayered films is similar. In both cases the cells connect to the surface with filopodia. The spreading of the cells was achieved through an intimate contact between cells and the surface of the films. Thus, abundant cytoplasmatic filopodias were detected forming bridges between the agglomerates of the material at the surface of the films.

As the serum used to culture cells contains a number of proteins, in addition to electrolytes, antibodies, antigens, etc., viability results discussed above may be simply due to the nonspecific binding between serum proteins and the CP. To corroborate the function of CREKA in the bioactivity of the composite, adhesion and proliferation assays were repeated culturing cells in a serum-free medium. Results, which have been expressed relative to the TCPS using a serum-containing culture medium, are included in Figures 7a and 7b, respectively. As it was expected, the relative viabilities obtained for the serum-free media decrease considerably with respect to those

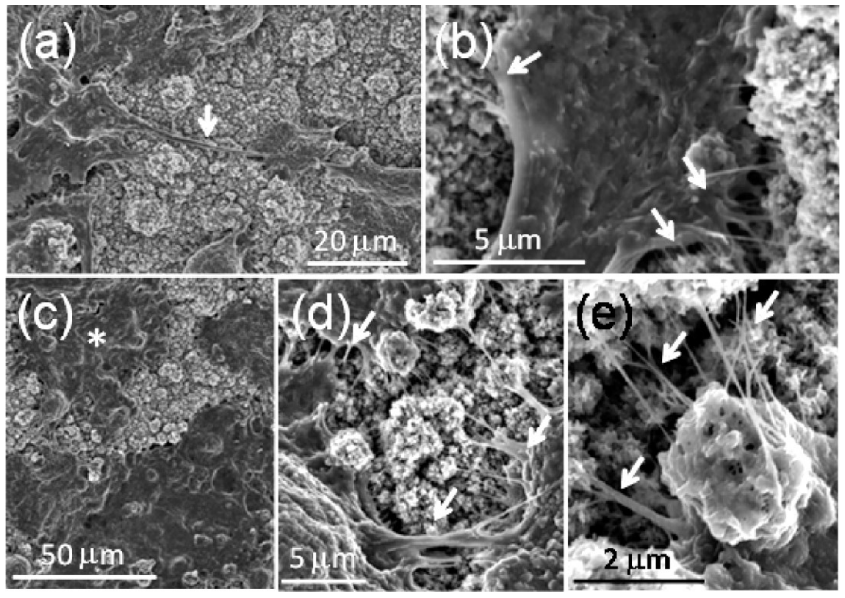

Figure 8. Adhesion and proliferation of DU-145 cells onto PEDOT(Acn+wat) (a,b) and PEDOT-CREKA(Acn+wat) (c–e) surfaces. (a) Clustered cells are connected by bridge cytoplasmatic elements (arrow), which is a prerequisite to colonize the material. (b) The cells spread filopodias (arrows) to adhere to the PEDOT(Acn+wat) surface. (c) Cells grouped in clusters (asterisk) to adhere to the PEDOT-CREKA(Acn+wat) surface. (d and e) The filopodias are the cytoplasmatic elements responsible for cellular adhesion to PEDOT-CREKA(Acn+wat).

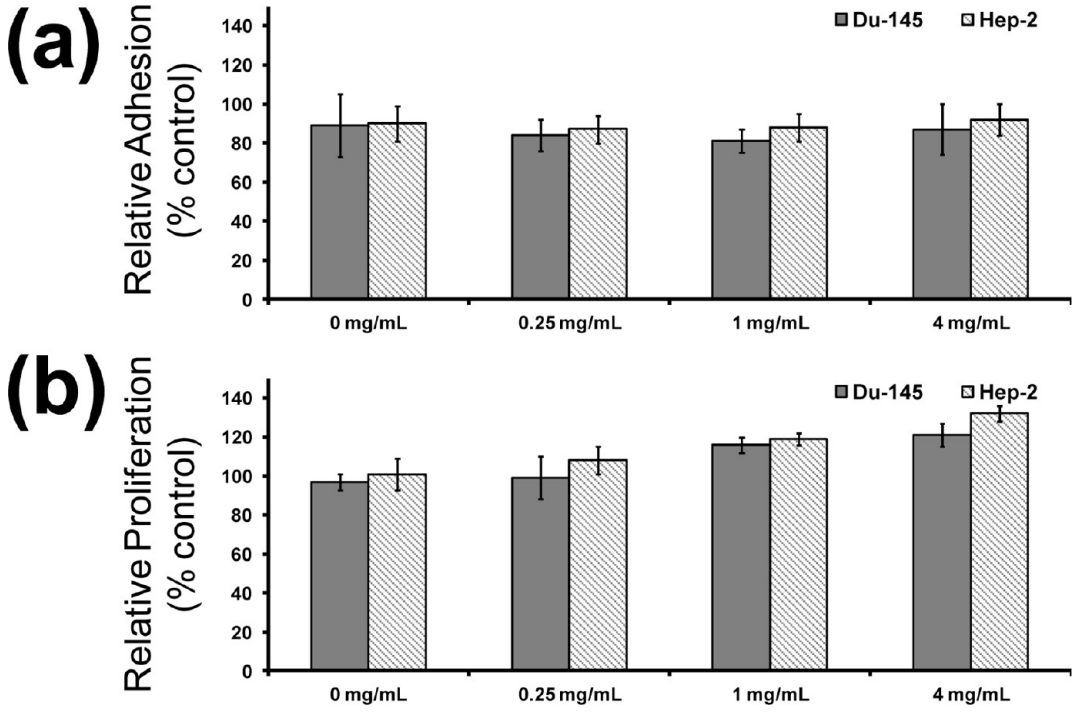

Figure 9. Cellular adhesion (a) and cellular proliferation (b) on the surface of PEDOT/PEDOT-CREKA(basic-wat) films prepared using 0.25, 1.0, and 4.0 mg/mL in the generation medium of the second layer. For comparison, results obtained for PEDOT/PEDOT(basic-wat) films (labeled as 0 mg/mL) are also displayed. Results are relative to the TCPS used as a control substrate in Figure 7. DU-145 and HEp-2 cells were cultured during 24 h (adhesion assay) and 7 days (proliferation assay), culture media being supplemented with fetal bovine serum in all cases (see Methods section). The experiments were performed using six samples for each substrate.

achieved in the serum-containing media in all cases. However, it is worth noting that the percentage of adhered and, specially, proliferated cells is greater for PEDOT/PEDOT-CREKA-(basic-wat) than PEDOT/PEDOT(basic-wat). The same finding is observed for PEDOT-CREKA(acid-wat) and PEDOT(acid-wat), even though the difference is less pronounced. These results allow us to verify the function of CREKA on cell binding.

Additional cell adhesion and proliferation assays were performed using PEDOT/PEDOT-CREKA(basic-wat) films prepared with a lower and higher concentration of peptide molecules. More specifically, the experimental conditions used to generate these films were identical to those described in the

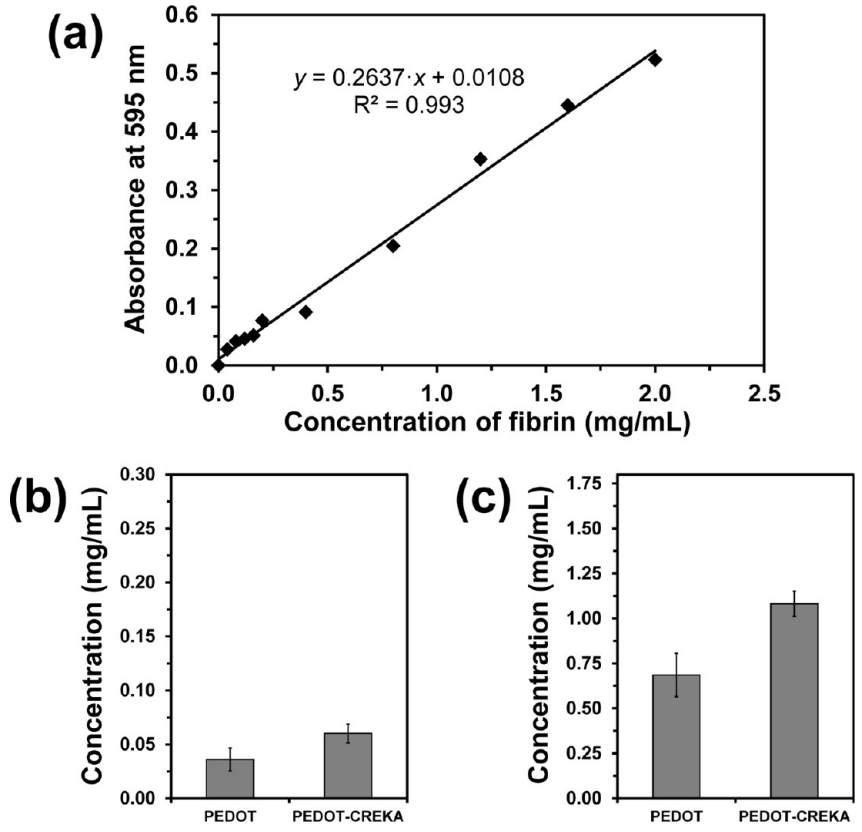

Figure 10. (a) Calibration curve representing the absorbance at 595 nm against the concentration of fibrin. The concentration of protein adsorbed by PEDOT/PEDOT(basic-wat) and PEDOT/PEDOT-CREKA(basic-wat) films when immersed in solutions with 2 and 10 mg/mL of fibrin are displayed in (b) and (c), respectively.

Methods section with the exception of the concentration of CREKA in the generation medium of the second layer, which changed from 1 mg/mL to 0.25 and 4 mg/mL. Cell assays were performed, supplementing the culture medium with fetal bovine serum, penicillin G, and streptomycin, as explained in the Methods section. Quantitative cellular adhesion and proliferation results are displayed in Figure 9. As was expected from results displayed in Figure 7, the influence of the peptide concentration in cellular adhesion is practically nonexistent (Figure 9a). In contrast, proliferation assays show that cell viability increases progressively with the concentration of peptide. Although such an increment is apparently moderate, it should be remarked that the proliferation is 24% (DU-145)/31% (HEp-2) higher for PEDOT/PEDOT-CREKA(basic-wat) prepared using 4 mg/mL of peptide than for PEDOT/PEDOT (basic-wat).

Binding of Fibrin. Assays to evaluate the adsorption of fibrin have been carried out using the composite prepared in a basic aqueous environment only, which showed the higher concentration of CREKA. Figure 10a represents the absorbance at the 595 nm−fibrin concentration calibration curve used to evaluate the ability of PEDOT/PEDOT-CREKA(basic-wat) to bind protein with respect to PEDOT/PEDOT(basic-wat), which has been used as blank.

The fibrin-binding capabilities of PEDOT/PEDOT(basic-wat) and PEDOT/PEDOT-CREKA(basic-wat) are compared in Figures 10b and 10c. Results provided by the binding assay using the 2 mg/mL fibrin PBS:NaOH (pH = 12.2) solution (Figure 9b) indicate that the affinity of PEDOT/PEDOT-CREKA(basic-wat) toward the proteins is 50% higher than that of PEDOT/PEDOT(basic-wat). However, the amount of fibrin recovered from the solution was extremely low in both cases (i.e., ∼2−3%). This situation changes drastically when samples are immersed in 10 mg/mL of fibrin PBS:NaOH alkaline solutions, the amount of protein adsorbed by PEDOT/PEDOT-CREKA(basic-wat) and PEDOT/PEDOT(basic-wat) being 10.8% and 6.9%. These results corroborate our previous assumption about the influence of CREKA in cellular proliferation. More specifically, the higher performance of PEDOT/PEDOT-CREKA(basic) as bioactive cellular platform (Figure 7b) is due to the binding between the peptide entrapped into the CP matrix and the binding of fibrin molecules from the culture medium, promoting cell proliferation.

To evaluate the influence of the pH on the fibrin-binding capabilities and, therefore, on the bioactive conformation of CREKA, additional assays were performed using a 2 mg/mL fibrin solution with pH = 7.4, which was obtained by adjusting the alkaline PBS:NaOH solution with HCl (see Methods section). Results (Figure S1, SI) were practically identical to those displayed in Figure 10b, suggesting that the conformation of CREKA is not altered by the pH reduction. This behavior is fully consistent with the entrapment of the peptide into the CP matrix, the conformation of CREKA molecules being constrained by polymer chains.

Biocompatibility of PEDOT/PEDOT-CREKA(basic) Treated with Fibrin. It is well-known that fibrin is a biocompatible material that promotes cellular adhesion and proliferation.[51] To evaluate an alternative strategy for the use of PEDOT/PEDOT-CREKA(basic-wat) as a biocompatible plat-

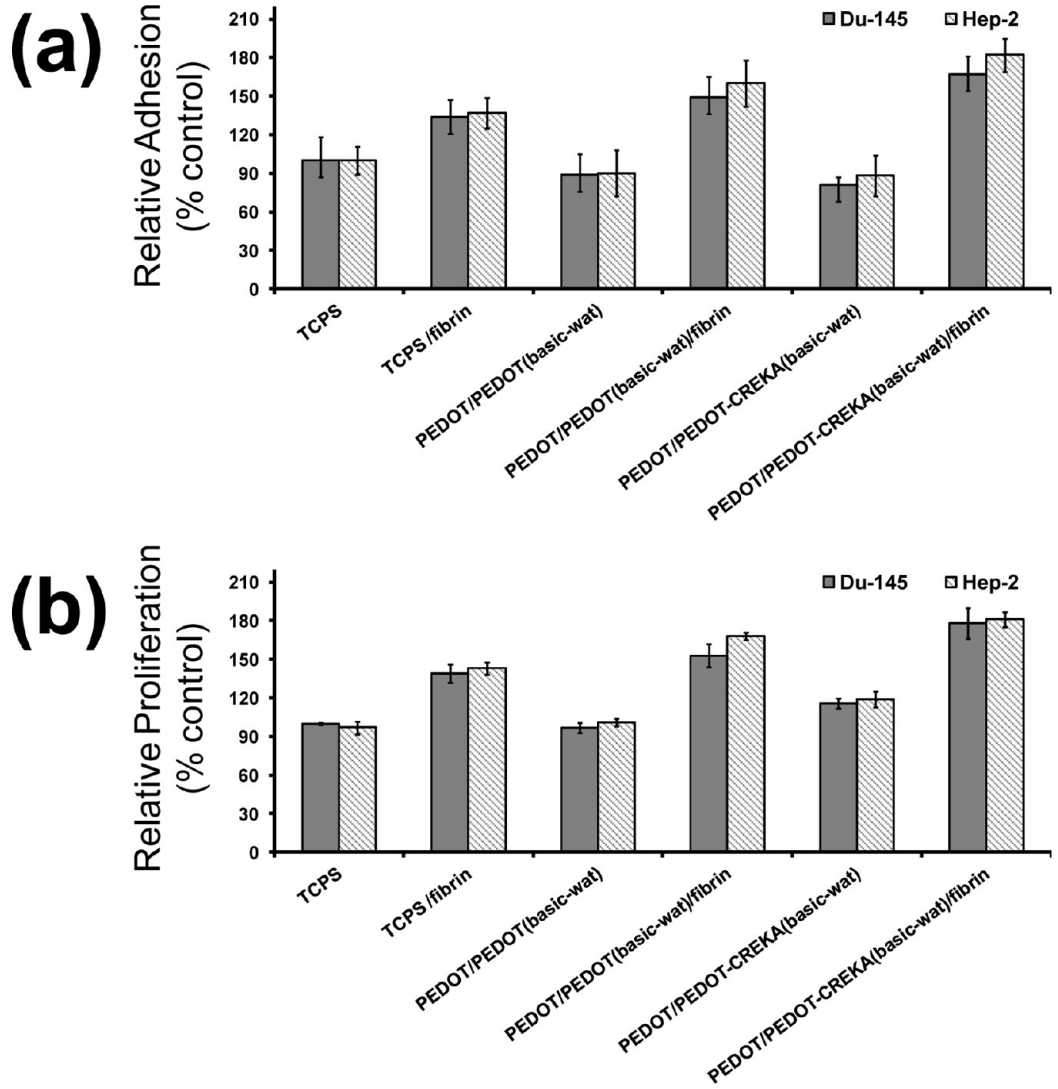

Figure 11. Cellular adhesion (a) and cellular proliferation (b) on the surface of PEDOT/PEDOT(basic-wat) and PEDOT/PEDOT-CREKA(basic-wat) treated with fibrin (see text). Results obtained for PEDOT/PEDOT(basic-wat) and PEDOT/PEDOT-CREKA(basic-wat) without any treatment have been included for comparison. DU-145 and HEp-2 cells were cultured during 24 h (adhesion assay) and 7 days (proliferation assay), culture media being supplemented with fetal bovine serum in all cases (see Methods section). Results are relative to TCPS without fibrin treatment. The experiments were performed using six samples for each substrate.

form, additional adhesion and proliferation assays were performed using PEDOT/PEDOT-CREKA(basic-wat) and PEDOT/PEDOT(basic-wat) films after adsorbing fibrin. More specifically, films obtained after immersion in 10 mg/mL of fibrin PBS:NaOH alkaline solutions (see previous subsection) were used for these assays. As it was mentioned above, the amount of protein adsorbed by PEDOT/PEDOT-CREKA(basic-wat) and PEDOT/PEDOT(basic-wat) was 10.8% and 6.9%, respectively. Results derived from cell adhesion and proliferation assays are displayed in Figure 11a and 11b, respectively, where the relative viabilities determined for films without fibrin have been also included for comparison. As it can be seen, fibrin promotes considerably cell adhesion and proliferation, this feature being particularly evident for PEDOT/PEDOT-CREKA(basic-wat). Thus, the cell viability grows with the concentration of adsorbed fibrin. According to these results, the affinity of CREKA toward fibrin can be employed to attach and grow cells directly onto the surface of the PEDOT/PEDOT-CREKA(basic-wat) composite or, alternatively, to create a very efficient bioactive platform treating the above-mentioned composite with fibrin before its use in cell regeneration applications.

CONCLUSIONS

PEDOT-CREKA composites have been prepared using different experimental conditions, which have been found to have a large impact not only on the content of entrapped peptide but also on the morphology and properties. The content of peptide has been determined to be relatively high in PEDOT/PEDOT-CREKA(basic-wat) bilayered films (i.e., one CREKA molecule per ~6 EDOT units) and very low for PEDOT-CREKA(acid-wat) and PEDOT-CREKA(Acn+wat) single-layered systems (i.e., one CREKA molecule per ~85 and >350 EDOT units).

The surface morphology of PEDOT/PEDOT-CREKA-(basic-wat) films consists of a homogeneous distribution of compact, relatively prominent, and well-localized folds, whereas PEDOT-CREKA(Acn+wat) and PEDOT-CREKA(acid-wat) surfaces present flake-like aggregates and clustered aggregates of thin fiber-like networks, respectively. These morphologies

result from the different polymerization conditions (i.e., solvent, pH, potential, dopant anion, and single- or bilayered structure), while entrapment of the peptide into the CP matrix does not affect the surface morphology. On the other hand, the influence of peptide in the electrochemical properties of the CP is very small for the biocomposites prepared using SDBS, the electroactivity and electrochemical stability of PEDOT/PEDOT-CREKA(basic-wat) being significantly higher than those of PEDOT-CREKA(acid-wat). In contrast, CREKA clearly reduces the electroactivity of PEDOT(Acn+wat), which has been attributed to the charge and large size of peptide molecules with respect to those of the perchlorate anions.

Results obtained in this work suggest that PEDOT/PEDOT-CREKA biocomposites could be used for different biomedical applications in which the integration of the intrinsic properties of PEDOT and the benefit induced by the peptides represent an advantage (e.g., implants for tissue engineering, nerve regeneration, and components for orthopedic devices). To increase even more the biocompatibility of PEDOT/PEDOT-CREKA, a strategy that takes advantage of the ability of the peptide to bind fibrin has been successfully explored. However, our most immediate objective consists of the preparation and characterization of bilayered biocomposites based on the combination of PEDOT and some recently developed CREKA analogues that were found to induce tumor necrosis.[22] Thus, such new biocomposites, which are being prepared using the same experiment as PEDOT/PEDOT-CREKA(basic-wat), are expected to add selective cellular response, increasing the range of potential biomedical applications.

■ ASSOCIATED CONTENT

Ⓢ Supporting Information

Details of the equipment and procedures (i.e., Methods section) used for the characterization of the prepared materials as well as for the biological assays. This material is available free of charge via the Internet at http://pubs.acs.org.

■ AUTHOR INFORMATION

Corresponding Author

*E-mail: carlos.aleman@upc.edu.

Notes

The authors declare no competing financial interest.

■ ACKNOWLEDGMENTS

This work has been supported by MICINN and FEDER funds (project number MAT2012-34498), by the DIUE of the Generalitat de Catalunya (contracts number 2009SGR925 and XRQTC). G.F. and B.T.D. thank the UPC and MICINN, respectively, for an FPI grant. Authors are indebted to Dr. D. Aradilla for his contribution to some SEM micrographs. Support for the research of C.A. was received through the prize "ICREA Academia" for excellence in research funded by the Generalitat de Catalunya.

■ REFERENCES

(1) Zhao, H. C.; Zhu, B.; Luo, S. C.; Lin, H. A.; Nakao, A.; Yamashita, Y.; Yu, H. H. Controlled Protein Absorption and Cell Adhesion on Polymer-Brush-Grafted Poly(3,4-ethylenedioxythiophene) Films. *ACS Appl. Mater. Interfaces* **2013**, *5*, 4536−4543.

(2) Zhao, H. C.; Zhu, B.; Sekine, J.; Luo, S. C.; Yu, H. H. Oligoethylene-Glycol-Functionalized Polyoxythiophenes for Cell Engineering: Syntheses, Characterizations, and Cell Compatibilities. *ACS Appl. Mater. Interfaces* **2012**, *4*, 680−686.

(3) Cui, X.; Martin, D. C. Fuzzy Gold Electrodes for Lowering Impedance and Improving Adhesion with Electrodeposited Conducting Polymer Films. *Sens. Actuators, A* **2003**, *103*, 384−394.

(4) Bendrea, A.-D.; Fabregat, G.; Cianga, L.; Estrany, F.; del Valle, L. J.; Cianga, I.; Alemán, C. Hybrid Materials Consisting of an All-Conjugated Polythiophene Backbone and Grafted Hydrophilic Poly(ethylene glycol) Chains. *Polym. Chem.* **2013**, *4*, 2709−2723.

(5) Guimard, N. K.; Gomez, N.; Schmidt, C. E. Conducting Polymers in Biomedical Engineering. *Prog. Polym. Sci.* **2007**, *32*, 876−921.

(6) Zhong, Y.; Yu, X.; Gilbert, R.; Bellamkonda, R. V. Stabilizing Electrode-Host Interfaces: A Tissue Engineering Approach. *J. Rehabil. Res. Dev.* **2001**, *38*, 627−632.

(7) Cui, X.; Wiler, J.; Dzaman, M.; Altschuler, R. A.; Martin, D. C. In Vivo Studies of Polypyrrole/Peptide Coated Neural Probes. *Biomaterials* **2003**, *24*, 777−787.

(8) Garner, B.; Hodgson, A. J.; Wallace, G. G.; Underwood, P. A. Human Endothelial Cell Attachment to and Growth on Polypyrrole-Heparin Is Vitronectin Dependent. *J. Mater. Sci.: Mater. Med.* **1999**, *10*, 19−27.

(9) Green, R. A.; Lovell, N. H.; Poole-Warren, L. A. Cell Attachment Functionality of Bioactive Conducting Polymers for Neural Interfaces. *Biomaterials* **2009**, *30*, 3637−3644.

(10) Cui, X. Y.; Martin, D. C. Electrochemical Deposition and Characterization of Poly(3,4-ethylenedioxythiophene) on Neural Microelectrode Arrays. *Sens. Actuators, B* **2003**, *89*, 92−102.

(11) Xiao, Y. H.; Cui, X. Y.; Hancock, J. M.; Bouguettaya, M.; Reynolds, J. R.; Martin, D. C. Electrochemical Polymerization of Poly(hydroxymethylated-3,4-ethylenedioxythiophene) (PEDOT−MeOH) on Multichannel Neural Probes. *Sensors Actuators, B* **2004**, *99*, 437−443.

(12) Sanghvi, A. B.; Miller, K. P.-H.; Belcher, A. M.; Schmidt, C. E. Biomaterials Functionalization Using a Novel Peptide that Selectively Binds to a Conducing Polymer. *Nat. Mater.* **2005**, *4*, 496−502.

(13) De Giglio, E.; Sabbatini, L.; Zambonin, P. G. Development and Analytical Characterization of Cysteine-Grafted Polypyrrole Films Electrosynthesized on Pt- and Ti-Substrates as Precursors of Bioactive Interfaces. *J. Biomater. Sci., Polym. Ed.* **1999**, *10*, 845−858.

(14) De Giglio, E.; Sabbatini, L.; Colucci, S.; Zambonin, G. Synthesis, Analytical Characterization, and Osteoblast Adhesión Properties on RGD-Grafted Polypyrrole Coating on Titanium Substrates. *J. Biomater. Sci., Polym. Ed.* **2000**, *11*, 1073−1083.

(15) Gomez, N.; Schmidt, C. E. Nerve Growth Factor-Immobilized Polypyrrole: Bioactive Electrically Conducting Polymer for Enhanced Neurite Extension. *J. Biomed. Mater. Res., Part A* **2007**, *81*, 135−149.

(16) Fabregat, G.; Ballano, G.; Armelin, E.; del Valle, L. J.; Cativiela, C.; Alemán, C. An Electroactive and Biologically Responsive Hybrid Conjugate Based on Chemical Similarity. *Polym. Chem.* **2013**, *4*, 1412−1424.

(17) Pasqualini, R.; Ruoslahti, E. In Vivo Using Phage Display Peptide Libraries. *Nature* **1996**, *380*, 364−366.

(18) Hoffman, J. A.; Giraudo, E.; Singh, M.; Zhang, L.; Inoue, M.; Porkka, K.; Hanahan, D.; Ruoslahti, E. Progressive Vascular Changes in a Transgenic Mouse Model of Squamous Cell Carcinoma. *Cancer Cell* **2003**, *4*, 383−391.

(19) Simberg, D.; Duza, T.; Park, J. H.; Essler, M.; Pilch, J.; Zhang, L.; Derfus, A. M.; Yang, M.; Hoffman, R. M.; Bathia, S.; Sailor, M. J.; Ruoslahti, E. Biomimetic Amplification of Nanoparticle Homing to Tumors. *Proc. Natl. Acad. Sci. U.S.A.* **2007**, *104*, 932−936.

(20) Zanuy, D.; Flores-Ortega, A.; Casanovas, J.; Curcó, D.; Nussinov, R.; Alemán, C. The Energy Landscape of a Selective Tumor-Homing Pentapetide. *J. Phys. Chem. B* **2008**, *112*, 8692−8700.

(21) Zanuy, D.; Curcó, D.; Nussinov, R.; Alemán, C. Influence of the Dye Presence on the Conformational Preferences of CREKA, a Tumor Homing Linear Pentapeptide. *Biopolymers* **2009**, *92*, 83−93.

(22) Agemy, L.; Sugahara, K. N.; Kotamraju, V. R.; Gujraty, K.; Girard, O. M.; Kono, Y.; Mattrey, R. F.; Park, J.-H.; Sailor, M. J.;

Jimenez, A. I.; Cativiela, C.; Zanuy, D.; Sayago, F. J.; Alemán, C.; Nussinov, R.; Ruoslahti, E. Nanoparticle-Induced Vascular Blockade in Human Prostate Cancer. *Blood* **2010**, *116*, 2847−2856.
(23) Wang, J. Y.; Chen, L. C.; Ho, K. C. Synthesis of Redox Polymer Nanobeads and Nanocomposites for Glucose Biosensors. *ACS Appl. Mater. Interfaces* **2013**, *5*, 7852−7861.
(24) Luo, S. C.; Xie, H.; Chen, N. Y.; Yu, H. H. Trinity DNA Detection Platform by Ultrasmooth and Functionalized PEDOT Biointerfaces. *ACS Appl. Mater. Interfaces* **2009**, *1*, 1414−1419.
(25) López-Pérez, D. E.; Aradilla, D.; del Valle, L. J.; Alemán, C. Capacitive Composites Made of Conducting Polymer and Lysozyme: Toward the Biocondenser. *J. Phys. Chem. C* **2013**, *117*, 6607−6619.
(26) Ocampo, C.; Oliver, R.; Armelin, E.; Alemán, C.; Estrany, F. Electrochemical Synthesis of Poly(3,4-ethylenedioxythiophene) on Steel Electrodes: Properties and Characterization. *J. Polym. Res.* **2006**, *13*, 193−200.
(27) Aradilla, D.; Estrany, F.; Azambuja, D. S.; Casas, M. T.; Puiggalí, J.; Ferreira, C. A.; Alemán, C. Conducting Poly(3,4-ethylenedioxythiophene)-Montmorillonite Exfoliated Nanocomposite. *Eur. Polym. J.* **2010**, *46*, 977−983.
(28) Sivakumar, C.; Phani, K. L. Nanocatalyst ∪ Reagent-on-a-Polymer Film" a New Polymer-Supported System for (Electro-)Catalytic Reactions. *Chem. Commun.* **2011**, *47*, 3535−3537.
(29) Liu, S.; Liu, H.; Bandyopadhyay, K.; Gao, Z.; Echegoyen, L. Dithia-Crown-Annelated Tetrathiafulvalene Disulfides: Synthesis Electrochemistry, Self-Assembled Films, and Metal Ion Recognition. *J. Org. Chem.* **2000**, *65*, 3292−3298.
(30) Kvarnstrom, C.; Neugebauer, H.; Blomquist, H.; Ahonen, H. J.; Kankare, J.; Ivaska, A. In Situ Spectroelectrochemical Characterization of Poly(3,4-ethylenedioxythiophene). *Electrochim. Acta* **1999**, *44*, 2739−2750.
(31) Garreau, S.; Louarn, G.; Buisson, J. P.; Froyer, G.; Lefrant, S. In Situ Spectroelectrochemical Raman Studies of Poly(3,4-ethylenedioxythiophene) (PEDT). *Macromolecules* **1999**, *32*, 6807−6812.
(32) Ahmad, S.; Deepa, M.; Singh, S. Electrochemical Synthesis and Surface Characterization of Poly(3,4-ethylenedioxythiophene) Films Grown in an Ionic Liquid. *Langmuir* **2007**, *23*, 11430−11433.
(33) Wang, G.-F.; Tao, X.-M.; Xin, J. H.; Fei, B. Modification of Conductive Polymer for Polymeric Anodes of Flexible Organic Light-Emitting Diodes. *Nanoscale Res. Lett.* **2009**, *4*, 613−617.
(34) Spanninga, S. A.; Martin, D. C.; Chen, Z. X-ray Photoelectron Spectroscopy Study of Counterion Incorporation in Poly(3,4-ethylenedioxythiophene) (PEDOT) 2: Polyanion Effect, Toluenesulfonate, and Small Anions. *J. Phys. Chem. C* **2010**, *114*, 14992−14997.
(35) Bhattacharyya, D.; Gleason, K. K. Single-Step Oxidative Chemical Vapor Deposition of −COOH Functional Conducting Copolymer and Immobilization of Biomolecules for Sensor Application. *Chem. Mater.* **2011**, *23*, 2600−2605.
(36) Stevens, J. S.; de Luca, A. C.; Pelendritis, M.; Terenghi, G.; Downes, S.; Schroeder, S. L. M. Quantitative Analysis of Complex Amino Acids and RGD Peptides by X-ray Photoelectron Spectroscopy (XPS). *Surf. Interface Anal.* **2013**, *45*, 1238−1246.
(37) Sakmeche, N.; Aeiyach, S.; Aaron, J.-J.; Jouini, M. Improvement of the Electrosynthesis and Physicochemical Properties of Poly(3,4-ethylenedioxythiophene) Using a Sodium Dodecyl Sulfate Micellar Aqueous Medium. *Langmuir* **1999**, *15*, 2566−2574.
(38) Flamia, R.; Lanza, G.; Salvi, A. M.; Castle, J. E.; Tamburro, A. M. Conformational Study and Hydrogen Bonds Detection on Elastin-Related Polypeptides Using X-Ray Photoelectron Spectroscopy. *Biomacromolecules* **2005**, *6*, 1299−1309.
(39) Strother, T.; Hamers, R. J.; Smith, L. M. Covalent Attachment of Oligodeoxyribonucleotides to Amine-Modified Si (001) Surfaces. *Nucleic Acids Res.* **2000**, *28*, 3535−3541.
(40) Iucci, G.; Dettin, M.; Battocchio, C.; Gambaretto, R.; Di Bello, C.; Polzonetti, G. Novel Immobilizations of an Adhesion Peptide on the TiO_2 Surface: An XPS Investigation. *Mater. Sci. Eng., C* **2007**, *27*, 1201−1206.
(41) Aradilla, D.; Azambuja, D.; Estrany, F.; Iribarren, J. I.; Ferreira, C. A.; Alemán, C. Poly(3,4-ethylenedioxythiophene) on Self-Assembled Alkanethiol Monolayers for Corrosion Protection. *Polym. Chem.* **2011**, *2*, 2548−2556.
(42) Moulder, J. F.; Stickle, W. F.; Sobol, P. E.; Bomben, K. D. In *Handbook of X-ray Photoelectron Spectroscopy: a Reference Book of Standard Spectra for Identification and Interpretation of XPS Data*; Perkin-Elmer Corporation: Eden Prairie, MN, 1995.
(43) Greczynski, G.; Kugler, T.; Salaneck, W. R. Characterization of the PEDOT-PSS System by Means of X-Ray and Ultraviolet Photoelectron Spectroscopy. *Thin Solid Films* **1999**, *354*, 129−135.
(44) Zotti, G.; Zecchin, S.; Schiavon, G. Electrochemical and XPS Studies Toward the Role of Monomeric and Polymeric Sulfonate Counterions in the Synthesis, Composition, and Properties of Poly(3,4-ethylenedioxythiophene). *Macromolecules* **2003**, *36*, 3337−3344.
(45) Taffarel, S. R.; Rubio, J. Adsorption of Sodium Dodecyl Benzene Sulfonate from Aqueous Solution Using a Modified Natural Zeolite with CTAB. *Miner. Eng.* **2010**, *23*, 771−779.
(46) Aradilla, D.; Estrany, F.; Alemán, C. Different Properties for Poly(3,4-ethylenedioxythiophene) Films Derived from Single or Multiple Polymerization Steps. *J. Appl. Polym. Sci.* **2011**, *121*, 1982−1991.
(47) Aradilla, D.; Estrany, F.; Armelin, E.; Alemán, C. Morphology and Growing of Nanometric Multilayered Films Formed by Alternated Layers of Poly(3,4-ethylenedioxythiophene) and Poly(N-methylpyrrole). *Thin Solid Films* **2010**, *518*, 4203−4210.
(48) Aradilla, D.; Estrany, F.; Armelin, E.; Alemán, C. Ultraporous Poly(3,4-ethylenedioxythiophene) for Nanometric Electrochemical Supercapacitor. *Thin Solid Films* **2012**, *520*, 4402−4409.
(49) Estrany, F.; Aradilla, D.; Oliver, R.; Alemán, C. Electroactivity, Electrochemical Stability and Electrical Conductivity of Multilayered Films Containing Poly(3,4-ethylenedioxythiophene) and Poly(N-methylpyrrole). *Eur. Polym. J.* **2007**, *43*, 1876−1882.
(50) Alemán, C.; Oliver, R.; Brillas, E.; Casanovas, J.; Estrany, F. A Combined Theoretical and Experimental Investigation about the Influence of the Dopant in the Anodic Electropolymerization of alpha-Tetrathiophene. *Chem. Phys.* **2006**, *323*, 407−412.
(51) De Faveri, S.; Maggiolini, E.; Miele, E.; De Angelis, F.; Cesca, F.; Benfenati, F.; Fadiga, L. Bio-Inspired Hybrid Microelectrodes: A Hybrid Solution to Improve Long-Term Performance of Chronic Intracortical Implants. *Front. Neuroeng.* **2014**, *7*, 1−12.